Submitted to the 29th International Conference on High-Energy Physics ICHEP98,
Vancouver, Canada, July 1998

Forward Jet and Particle Production in Deep Inelastic Scattering at low Bjorken-x at HERA

H1 Collaboration

Abstract

Single particles and jets in deep inelastic scattering at low x are measured with the H1 detector in the region between the current jet and the proton remnant, termed the forward region. This region is expected to be particularly sensitive to QCD evolution effects. The forward single and di-jet cross sections are presented for jets produced with an angle, θ, with respect to the proton direction in the range $7^\circ < \theta < 20^\circ$ and with transverse momenta, p_T, greater than 3.5 GeV. Charged and neutral single particle production in the forward region is studied in the range $5^\circ < \theta < 25^\circ$ and for p_T larger than 1 GeV. The results are compared to QCD based Monte Carlo predictions and analytical calculations based on BFKL evolution and next to leading order QCD.

Abstract: 529
Parallel sessions: 3
Plenary sessions: 5

1 Introduction

The positron-proton collider HERA has significantly increased the available kinematic region for the study of deep inelastic scattering (DIS) towards large four-momentum transfer Q^2 (up to $Q^2 \approx 10^4$ GeV^2) and small Bjorken-x ($x \approx 10^{-4}$). The hadronic final state in such events is a very sensitive environment in which to disentangle different QCD processes. In particular the region near the proton remnant (forward region) will allow new insights to be gained into dynamical features of QCD at low Bjorken-x [1] since it provides a large phase space for parton emissions. Several prescriptions for the QCD evolution of the dynamics of such emissions have been proposed.

DGLAP [2] evolution in which the relevant evolution parameter is $\log(Q^2/Q_0^2)$ and in which emitted partons are strongly ordered in transverse momentum, k_T, has been successfully tested over wide ranges in Q^2 and provides, for instance, a good description of the structure function scaling violations. The BFKL [3] evolution equation, where the relevant evolution parameter is $\log(1/x)$ and for which there is no ordering in partonic k_T, is expected to become applicable at small enough x when the $\log(1/x)$ terms dominate the evolution. CCFM [4] evolution, in which the parton emissions obey angular ordering, is expected to be valid for both low and high Bjorken-x thereby forming a bridge between the BFKL and DGLAP approaches. Hadronic final state calculations for all three prescriptions are, for the first time, becoming available [5].

It has been noted that another approach based on a resolved photon component in deep inelastic scattering can emulate the random walk behaviour in k_T observed in the BFKL approach [6]. The resolved photon picture can be considered to be applicable when the squared transverse momentum of the parton of the hard scattering process is larger than Q^2 of the photon. In that case the photon can be considered to interact via its hadronic structure.

A complication in using the hadronic final state to investigate QCD evolution is the effect of soft hadronization processes and it has been suggested that these can be reduced by studying forward jet production [7, 8, 9]. Single high-p_T particle production has also been proposed as a probe of QCD dynamics [10, 11], the advantage of which, compared to jets, is the lack of dependence on the choice of jet finding algorithm and also the potential to reach smaller angles than is possible with jets with broad spatial extent. Previous measurements [12] on charged particle production which exploit this feature have been limited by experimental acceptance mostly to the central region of the detector.

In this analysis data from the H1 experiment are used to study the production of di-jets and high transverse momentum π^0-meson and charged particles in the forward region at small Bjorken-x.

2 Data Selection

Experimental data for this analysis were collected by H1 during the 1994 running period during which HERA collided 27.5 GeV positrons on 820 GeV protons. Integrated luminosities of the data samples used for the jets, π^0 and charged particle measurements are 2.8, 2.0 and 1.16 pb^{-1} respectively. These differences arise due to the importance of selecting running periods with optimal experimental conditions for each of the measurements presented here. DIS events are selected via the scattered positron in the H1 Backward Electromagnetic Calorimeter and are required to have $E_e^{'} > 12$ GeV (particles), $E_e^{'} > 11$ GeV (jets), $156^\circ < \Theta_e < 173^\circ$

(particles), $160° < \Theta_e < 173°$ (jets) and $y_e > 0.1$. Here $E_e^{'}$ and Θ_e are the energy and polar angle (with respect to the incoming proton direction) of the scattered positron respectively. Further reduction of photoproduction background from the DIS sample and the removal of events in which an energetic photon is radiated off the incoming positron is achieved by requiring $\sum_j (E_j - p_{z,j}) > 35$ GeV with the sum extending over all tracks and calorimeter clusters, j, in the event and avoiding double counting. The kinematic variables are determined using information from the scattered positron: $Q^2 = 4E_eE_e^{'}\cos^2(\Theta_e/2)$ and $y_e = 1 - (E_e/E_e^{'})\sin^2(\Theta_e/2)$. The scaling variable Bjorken-x is related to these quantities via the square of the centre of mass energy s: $x = Q^2/(ys)$.

2.1 Forward π^0-mesons

The π^0-mesons are measured in the dominant decay channel $\pi^0 \rightarrow \gamma\gamma$. The π^0 candidates are selected in the region $5° < \Theta_\pi < 25°$ using the finely segmented H1 Liquid Argon (LAr) calorimeter, where Θ_π is the polar angle of the produced π^0 with respect to the incoming proton beam direction. Candidates are required to have an energy of $E_\pi > 8$ GeV with a transverse component $E_{T,\pi} = E_\pi \sin\Theta_\pi > 1$ GeV. At the high π^0 energies considered here the two photons cannot be separated but appear as one object (cluster) in the calorimeter.

Photon induced showers are selected by measuring the shower shapes of candidate clusters. The selection criteria are based on the compact nature of electromagnetic showers as opposed to those of hadronic origin. The very fine segments ($\sim$ 44000 cells in total, with a cell size of 3.5 x 3.5 cm^2 and four-fold longitudinal segmentation in the forward region) of the H1 LAr calorimeter make possible a detailed study of the transverse and longitudinal spread and the energy distribution of each cluster.

The main difficulty of this analysis is the high particle density in the forward direction which leads to overlapping showers of electromagnetic and hadronic origin. Candidates of this type are mostly rejected. This high multiplicity of particles makes the use of track information as a rejection criterion unfeasible for the π^0 selection. Monte Carlo studies using a detailed simulation of the H1 detector nevertheless show the detection efficiency for π^0-mesons in the above specified region to be greater than 40% and predict that more than 75% of the selected candidate showers stem from π^0-mesons. The contribution of candidates not associated with the primary vertex is below 10%. The fraction of photons originating from the primary vertex and not produced via π^0 decays is estimated to be less than 2% [13].

2.2 Forward Charged Particles

Charged particles (cp) are selected using the forward (FT) and central (CT) tracking chambers. Basic quality criteria are used to select well measured tracks originating from the primary interaction point. For tracks restricted to the kinematic range used in this analysis: $p_{cp} > 8$ GeV, $p_{T,cp} > 1$ GeV, $5° < \Theta_{cp} < 25°$, over 90% are reconstructed in the FT. For this measurement, as for the π^0-mesons, the high particle multiplicity in the forward direction constitutes the main challenge. It gives rise to a large flux of soft particles produced in secondary interactions in passive material within the detector leading to a degradation of detection efficiency and resolution. The efficiency for reconstructing a central track and associating it to the primary event vertex is over 95% [14]. The equivalent forward track efficiency is over 40% [15] for tracks well contained within the FT. For tracks produced at low values of Θ_{cp} ($\Theta_{cp} < 10°$) a lower efficiency of 25% is obtained. The proportion of these selected charged particles produced in secondary interactions in passive material is negligible for central tracks but is estimated to be no more than 10% for the forward sample used here.

2.3 Forward Jet and Di-jet Selection

A cone algorithm is used to find jets in the H1 LAr calorimeter requiring an E_T larger than 3.5 GeV in a cone of radius $R = \sqrt{\Delta\eta^2 + \Delta\phi^2} = 1.0$ in the space of pseudo-rapidity η and azimuthal angle ϕ in the HERA frame of reference. Forward jets are selected according to the criteria $x_{\rm jet} = E_{\rm jet}/E_p > 0.035$, $0.5 < p^2_{T\rm jet}/Q^2 < 2$, $7^\circ < \Theta_{\rm jet} < 20^\circ$ and $p_{T\rm jet} > 3.5$ GeV, where $E_{\rm jet}$ and $p_{T\rm jet}$ are the energy and transverse momentum of the jet respectively and E_p is the incident proton energy. The cut $0.5 < p^2_{T\rm jet}/Q^2 < 2$ is designed to suppress hard emissions from DGLAP evolution and thus enhance sensitivity to any BFKL effects.

3 Results

3.1 Single Particles

Results are presented as spectra in Bjorken-x of π^0-mesons with $5^\circ < \Theta_\pi < 25^\circ$ and $p_{T,\pi} > 1$ GeV. The data are shown in Fig. 1 for the four different lower thresholds of $x_\pi >$ $[\ 0.0098,\ 0.012,\ 0.015,\ 0.017\ ]$ to illustrate the dependence on $x_\pi = E_\pi/E_{proton}$. All distributions shown are corrected bin-by-bin for detector effects and QED radiation. The full errors are the quadratic sum of the statistical (inner error bars) and systematic uncertainties. All distributions are normalized to the number of DIS events, N, that fall into the kinematic range: $E^{'}_e > 12$ GeV, $156^\circ < \Theta_e < 173^\circ$, $y_e > 0.1$ and $0.0002 < x_{bj} < 0.00236$. The data clearly rise with decreasing Bjorken-x providing evidence of much more hard partonic radiation than predicted by DGLAP type QCD models as represented by LEPTO [16]. A reasonable description of the data can be obtained by adding contributions from processes in which the photon is not point-like but acts as a resolved object as is implemented in RAPGAP [17]. The renormalisation and factorisation scales were both set to $p_T^2 + Q^2$ in these calculations where p_T^2 is the transverse momentum squared of the outgoing partons from the hard sub-process. For the first time the data can also be compared to a MC model based on the CCFM approach (LDCMC [5]). Although it is close to the data for the low x_π cutoffs it becomes increasingly similar to the DGLAP based model towards higher π^0 energies. The Color Dipole Model as implemented in ARIADNE [18] tends to overshoot the data in most of the measured distributions. BFKL calculations, folded with fragmentation functions, are available for the highest momentum π^0 bins [13]. These predictions were found to over-estimate the observed π^0 yield and the calculated points are shown in Fig. 1 divided by two. Despite this large normalisation discrepancy the calculations are seen to describe well the x dependence of the π^0 measurements.

Owing to the lower resolution of the FT with increasing p_T charged particle spectra are only currently presented for the lowest threshold of $x_{cp} = E_{cp}/E_{proton} > 0.0098$ used in the π^0-meson analysis. These results are shown in Fig. 2 (left). Both the data and the QCD models show the same Bjorken-x behavior as the π^0-meson spectra. To further check the consistency of both measurements ARIADNE with JETSET [19] was used to estimate the contribution of charged pions to the charged particle data. The results divided by two are compared to the π^0 measurement in Fig. 2 (right) and are in good agreement.

Event Sample	Forward 2-jet cross-section / pb
H1 Preliminary 1994 Data	$6.0 \pm 0.8 \pm 3.2$
ARIADNE	5.9
RAPGAP	6.0
LEPTO	2.8
LDC	1.6

Table 1: H1 Preliminary data and QCD calculations for forward di-jet events, with each jet satisfying $x_{\rm jet} = E_{\rm jet}/E_p > 0.035$, $0.5 < p^2_{T\rm jet}/Q^2 < 2$, $7^\circ < \Theta_{\rm jet} < 20^\circ$ and $p_{T\rm jet} > 3.5$ in the kinematic range $E_e^{'} > 11$ GeV , $156^\circ < \Theta_e < 173^\circ$ and $y_e > 0.1$.

3.2 Forward Jet and Di-jet Production

The forward jet selection described above yields 52 events with two jets satisfying the forward jet criteria. After the application of corrections for detector effects, the forward di-jet cross-section has been evaluated as $6.0 \pm 0.8(stat.) \pm 3.2(syst.)$ pb or roughly 1% of the forward jet cross section. The systematic error of this measurement is dominated by the uncertainty for the hadronic energy scale and model dependence of the correction procedure.

Recent numerical BFKL calculations at the parton level [20] predict that a fraction of 3 to 6% of the forward jet data should contain 2 or more forward jets. Table 1 compares the forward 2-jet cross-section in data with a number of QCD models with only ARIADNE and RAPGAP giving reasonable descriptions and LEPTO and the LDC failing to match the data.

This failure of the DGLAP approach to describe the forward di-jet cross-section is also observed in results on forward single jet production from the ZEUS [21] and H1 [22] collaborations. Fig. 3 shows the H1 Preliminary single jet cross-section as a function of x. Event and jet selection criteria for this analysis are the same as for the di-jet studies presented here. Several QCD-based models are compared to the data. LEPTO underestimates the cross-section while predictions from RAPGAP with a resolved photon contribution and ARIADNE are closer to the data. Numerical BFKL calculations at the parton level [23] lie above the data although they describe well the shape of the distribution. Exact NLO parton calculations from DISENT [24] using DGLAP parton densities are far from the data in both shape and normalisation. Further details of this analysis can be found in [22].

4 Summary

Measurements of single and di-jet cross-sections and high transverse momentum single particle rates in DIS in the forward region have been presented. Models based on DGLAP and CCFM evolution provide insufficient hard QCD radiation to match the data. Predictions from ARIADNE give a good description of the data as do those from RAPGAP which includes a resolved photon component. Analytical BFKL calculations over-estimate the yield of forward jets and single particles but provide a good description of the shape of their x dependence.

References

[1] A.H. Mueller, Nucl. Phys. B (Proc. Suppl.) 18C (1990) 125;
A.H. Mueller, J. Phys. G17 (1991) 1443;
J. Kwieciński, A.D. Martin, P.J. Sutton, Phys. Lett. B325 (1994) 212.

[2] Yu. L. Dokshitzer, Sov. Phys. JETP 46 (1977) 641;
V.N. Gribov, L.N. Lipatov, Sov. J. Nucl. Phys. 15 (1972) 438 and 675;
G. Altarelli, G. Parisi, Nucl. Phys. 126 (1977) 297.

[3] E.A. Kuraev, L.N. Lipatov, V.S. Fadin, Sov. Phys. JETP 45 (1972) 199;
Y.Y. Balitsky, L.N. Lipatov, Sov. J. Nucl. Phys. 28 (1978) 282.

[4] M. Ciafaloni, Nucl. Phys. B296 (1987) 259;
S. Catani, F. Fiorani, G. Marchesini, Phys. Let. 234B (1990) 339;
S. Catani, F. Fiorani, G. Marchesini, Nucl. Phys. B336 (1990) 18.

[5] W.J. Stirling, hep-ph/9804431.
G. Salam, hep-ph/9805322.
L. Lönnblad, JHEP 03 (1998) 006; hep-ph/9709424.

[6] H. Jung, L. Jönsson, H. Küster, DESY 98-051.

[7] A.H. Mueller, Nucl. Phys. B (Proc. Suppl.) 18C (1990) 125;
J. Phys. G17 (1991) 1443.

[8] J. Kwieciński, A.D. Martin, P.J. Sutton, Phys. Rev. D46 (1992) 921.

[9] J. Bartels, A. De Roeck, M. Loewe, Z. Phys. C54 (1992) 635;
W.K. Tang, Phys. Lett. B278 (1992) 363.

[10] M. Kuhlen, Phys. Lett. B382 (1996) 441.

[11] J. Kwiecinski, S.C. Lang and A.D. Martin, hep-ph/9707240.

[12] H1 Collab., C.Adloff et al., Nucl. Phys. B485 (1997) 3.

[13] J. Kwiecinski, S.C. Lang, A.D. Martin, Phys. Rev. D55 (1997) 1273.

[14] H1 Collab., S. Aid et al., Z. Phys. C72 (1996) 573.

[15] S. Burke et al., Nucl. Instr. and Meth. , A373 (1996) 227.

[16] G. Ingelman, A. Edin, J. Rathsman, Comp. Phys. Comm. 101 (1997) 108.

[17] H. Jung, Comp. Phys. Comm. 86 (1995) 147
`http://www-h1.desy.de/ jung/rapgap.html`

[18] L. Lönnblad, Comp. Phys. Comm. 71 (1992) 15.

[19] T. Sjöstrand, Comp. Phys. Comm. 39 (1986) 347;
T. Sjöstrand and M. Bengtsson, Comp. Phys. Comm. 43 (1987) 367.

[20] J. Kwiecinski, C.A.M. Lewis and A.D. Martin, Phys. Rev. D57 (1998) 496.

[21] ZEUS Collab., J. Breitweg et al., DESY 98-050, submitted to Eur. Phys. J..

[22] H1 Collab., S. Aid et al., Contributed paper pa 03-49, to ICHEP96, Warsaw, Poland, July 1996.

[23] J. Bartels et al., Phys. Lett. B384 (1996)300.

[24] S. Catani, M.H. Seymour,Nucl. Phys. B485 (1997) 291, Erratum-ibid.B510 (1997) 503.

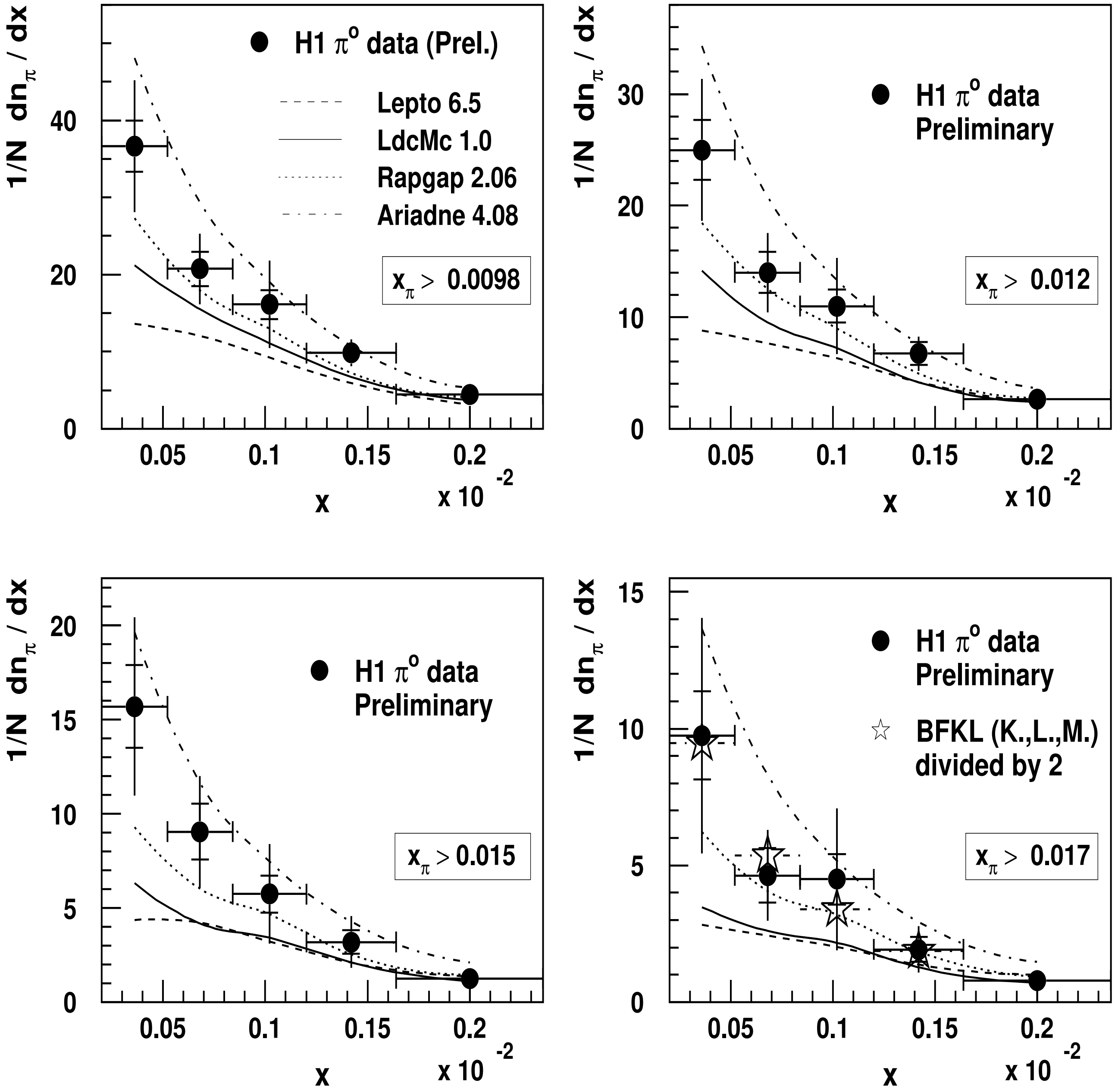

Figure 1: The forward π^0 spectra in Bjorken-x for $p_{T,\pi} > 1$ GeV and $5^\circ < \Theta_\pi < 25^\circ$ are shown for four different values of the lower threshold $x_\pi = E_\pi/E_{proton}$. Here n_π is the number of π^0-mesons and N is the number of events that enter the distribution. For comparison, predictions of four different QCD models are overlayed. For the lower two plots a BFKL calculation is available [13]. Its predictions have been divided by two for presentation.

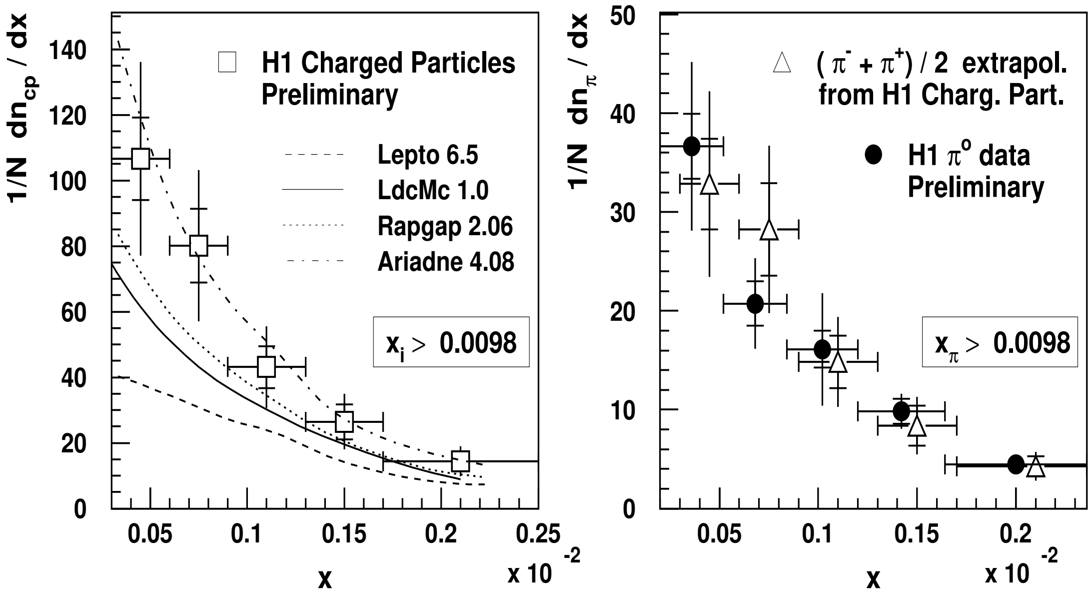

Figure 2: The forward charged particle spectra in Bjorken-x (left) and π^0-mesons (right) in the kinematic range $p_T > 1$ GeV, $5° < \theta < 25°$ and E >8 GeV. Here n_{cp} (n_π) is the number of charged particles (π^0-mesons) and N is the number of events that enter the distribution. The contribution of charged pions to the charged particle measurement as calculated by ARIADNE with JETSET is also shown (right). For comparison, predictions from four different Monte Carlo models are presented.

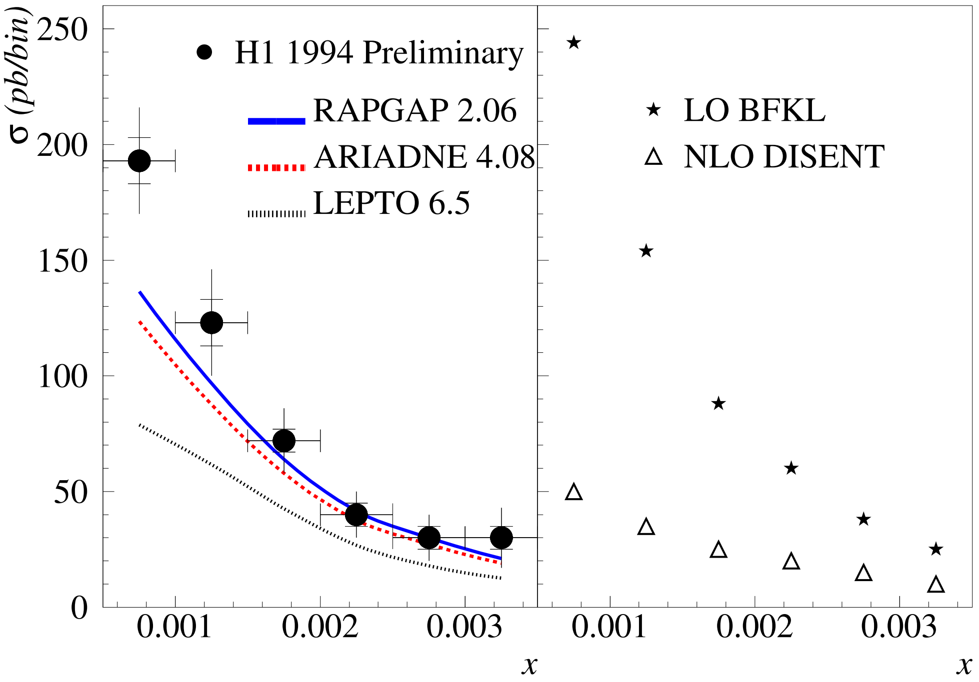

Figure 3: H1 Preliminary cross-sections and QCD calculations for inclusive forward jets satisfying $x_{\mathrm{jet}} = E_{\mathrm{jet}}/E_p > 0.035$, $0.5 < p_{T\mathrm{jet}}^2/Q^2 < 2$, $7° < \Theta_{\mathrm{jet}} < 20°$ and $p_{T\mathrm{jet}} > 3.5$.